

# STUDY OF THE INFLUENCE OF DESIGN PARAMETERS AND INITIAL CONDITION ON PASSIVE CONTAINMENT COOLING SYSTEM

**Yan WANG<sup>1\*</sup>, Yaoli ZHANG, Zhiwei ZHOU, Heng XIE**

Institute of Nuclear and New Energy Technology of Tsinghua University, the key laboratory of advanced reactor engineering and safety, Ministry of Education, Beijing, 100084, China

\*E-mail: wangyanfcw@tsinghua.edu.cn, Tel: +86-10-62788157.

**Yanning YANG,**

State Nuclear Power Technology Research and Development Centre, Beijing, 100190, China

## ABSTRACT

The passive containment cooling system, which only utilizes natural phenomena to remove the energy released from the reactor during the postulated accident to prevent the steel containment from overpressure, was designed and applied in the advanced 3rd generation pressurized water reactor. It is significant to study and evaluate the performance of passive containment cooling system. A dedicated analysis code PCCSAP-3D for the evaluation on the performance of passive containment cooling system is introduced briefly in this paper, and used to calculate the thermal-hydraulic transients in the containment of the advanced pressurized water reactor AP1000. The analyses on some key factors are studied and compared. The results show that the free volume of the containment and the thickness of the containment shell will be dominant for the transient pressure in containment during the postulated accident than the initial conditions, and the initial conditions in the containment is more sensitive than the ambient initial conditions.

## KEYWORDS:

passive containment cooling system; analysis code; advanced PWR; sensitivity

## 1. INTRODUCTION

With more focus on the reactor safety, in the current design on the safety system of the advanced reactor, some essentially passive means are provided.

As one of the main passive safety systems in the advanced pressurized water reactor (APWR), the concept of the passive containment cooling system (PCCS) is applied currently, which removes decay heat effectively and cools the reactor after a postulated design basis accident (DBA) to avoid containment heat-up and overpressure, such as loss-of-coolant accident (LOCA) and main steam line break (MSLB) [1, 2].

The passively cooled containment as the main part of the PCCS operating under the postulated accidents is illustrated as Figure 1[1].

With provisions of water spray from Passive Containment Cooling Water Storage Tank (PCCWST) driven by gravity in passive means, the external surface of the containment steel shell is wetted and a water film will form on it. During the water-film flowing along the surface from top to bottom, the containment is cooled by water evaporation. The concrete shield building surrounds the shell, and an outlet(chimney) on top of the concrete shield building is used to vent steam. An annular space between the containment shell and the concrete shield building provides a flow channel for the air. Air enters the annular space through the inlets located at the upper part of the shield building wall, then rises in the annulus and develops into natural draft as the air is heated by the containment surface. Finally, the heated air exits the shield building through the chimney. The external heat transfer of the water film can be enhanced by the convection between the thin water film on the outside containment surface and the air in the annular space. Some heat is also removed from the shield building surfaces by natural convection and by condensation on its wetted surfaces. In addition, a part of heat is transferred from the containment shell to the adjacent surface of air baffle by radiation, but it is not dominating because of the limited temperature. Thus, through a heat transfer path including steam condensation and convection on the internal surface of the containment shell, heat conduction of steel containment shell, convection and evaporation of the water film on the external surface of the containment shell, convection and condensation on the air baffle, convection of the concrete shield building and wall-to-wall radiation, the passively cooled steel containment utilizes only natural phenomena to remove the energy released from the reactor to avoid the overpressure of the containment during the postulated accident.

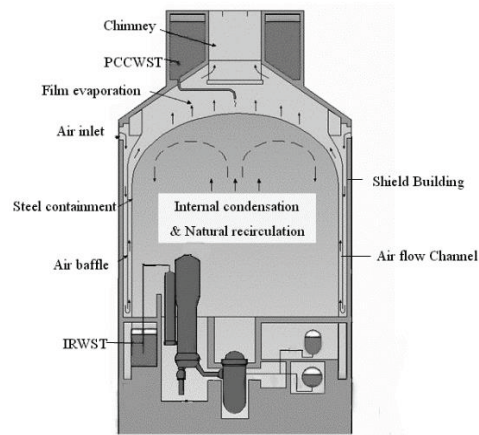


**Figure 1. Illustration of PCCS**

The thermal-hydraulic transient in the containment under the postulated accident is dominated by the PCCS performance. The transient peak pressure in the containment, as the most important parameter for the evaluation on the PCCS performance, is affected by many factors, such as free volume of containment, the temperature and the humidity in containment, the environment temperature, and so on. Therefore, it is mandatory to research and evaluate the reliance of the PCCS performance. Because of the immense cost of experimental research, numerical simulations have been rapidly developed. Some existing thermal- hydraulic codes are chosen to develop for the PCCS analysis, such as GOTHIC[3], CONTEMP4/MOD5[4], COMMIX[5], which were the ones reviewed to meet most closely the requirements identified in the Phenomena Identification and Ranking Table (PIRT) of the PCCS, although none of the codes met all of the requirements. Some models were modified and supplemented in the analysis codes to describe the special dominant characters of the PCCS during the transients. With associated nodding structure combined into GOTHIC to model the special heat and mass transfer on the PCCS, the modified code of Westinghouse-GOTHIC (WGOthic) was developed for the PCCS analysis on the Westinghouse APWR[6]. The WGOthic code was validated with the numerical solutions to the specified standard problems, the separate effects test and the integral test for AP600 and AP1000. The result shows good agreement which indicates the WGOthic has the enough capability for the evaluation on the PCCS performance. The advanced pressurized water reactor AP1000 under the postulated Cold-leg LOCA and the MSLB were analyzed by WGOthic code [7], and the results indicate the

pressure in the containment during the accident transient is controlled under design limitation and the containment is cooled effectively by the PCCS performance.

Based on the “Important National Science & Technology Specific Projects” of China, several units of APWR were imported, and the technology of large advanced pressurized water reactor is mastered, improved and re-innovated. For the design of large APWR in China in the future, an analysis code PCCSAP-3D was designed and developed for the PCCS analysis. The PCCSAP-3D was validated by the comparison with COMMIX on the AC600 [8] and the comparison with the WGOthic code on the AP1000 under the postulated DBAs[9]. The good agreement on the results shows the applicability of the new code on the PCCS analysis. In this paper, PCCSAP-3D is used for the study on the PCCS performance of AP1000. For better understanding, it is introduced briefly in the next section.

## 2. PCCSAP-3D

### 2.1. General Description on PCCSAP-3D

With the cooperation of State Nuclear Power Technology Research and Development center (SNPTRD) and Tsinghua University in China, a transient analysis code PCCSAP-3D was developed for the evaluation on the PCCS performance of the large APWR, which can simulate the transient response in the containment with the PCCS performance under the postulated DBAs.

The PCCSAP-3D code is a three-dimensional thermal hydraulic analysis code using separated field equations for three phase flow with multiple gas components. The analytical models used in the code were similar to those used in the PCCSAC code [8], which was developed to analyze the containment cooling system of AC600. The conventional Alternating Direction Implicit (ADI) method is improved with the Pre-conditioned General Minimum Residual (GMRES) method for better solution of pressure equation, because the latter is more efficient than the former in solving the structural and sparse pressure coefficient matrix, especially as the pressure coefficient matrix is large. The equations were deduced from the implicit difference equations of mass and momentum [10].

### 2.2. Basic Governing Equations for Fluid

The basic field model in the PCCSAP-3D is based on fundamental conservation principles: mass, momentum and energy conservation equations, which classifies the fluid into steam, noncondensable air, continuous liquid water and discontinuous water.

The nine-equation model including the  $k$ - $\epsilon$  turbulence model and a diffusion model are considered in the PCCS analysis code.

Mass conservation of the continuous liquid water is described as

$$\frac{\partial}{\partial t} [(1 - \alpha)\rho_l] + \nabla \cdot [(1 - \alpha)\rho_l \mathbf{u}_l] = -\Gamma + G_l + \dot{m} \psi \quad (1)$$

Where  $\alpha$  is the gas volume fraction,  $\rho_l$  is the liquid density,  $\mathbf{u}_l$  is the liquid velocity vector,  $\Gamma$  is the liquid evaporation rate,  $G_l$  is the inlet liquid mass flow rate from the pipe break into the containment,  $\dot{m}$  is the condensation rate on the wall, and  $\psi$  is the wall area per unit cell volume.

Mass conservation of steam

$$\frac{\partial}{\partial t} [\alpha \rho_s] + \nabla \cdot [\alpha \rho_s \mathbf{u}_g] + \alpha D \nabla \cdot (-\nabla \rho_s) = \Gamma + G_s - m \psi \quad (2)$$

Where  $\rho_s$  is steam density,  $\mathbf{u}_g$  is gas velocity vector,  $D$  is diffusion coefficient between the air and the steam,  $G_s$  is the inlet mass flow rate of steam from the pipe break into the containment.

Mass conservation of noncondensable air

$$\frac{\partial}{\partial t} [\alpha \rho_a] + \nabla \cdot [\alpha \rho_a \mathbf{u}_g] + \alpha D \nabla \cdot (-\nabla \rho_a) = G_a \quad (3)$$

Where,  $\rho_a$  is the noncondensable air density,  $G_a$  is the mass flow rate of the noncondensable air which is entrained with water from the pipe break into the containment.

For the assumption that the noncondensable air and the steam have the same velocity, the momentum conservation equation for the mixture of air and steam will be written as

$$\frac{\partial}{\partial t} [\alpha \rho_g \mathbf{u}_g] + \nabla \cdot [\alpha \rho_g \mathbf{u}_g \mathbf{u}_g + \alpha \Sigma] = \alpha \rho_s \mathbf{g} + \Gamma \mathbf{u}_{gl} - m \psi \mathbf{u}_g + G_s \mathbf{u}_{Gs} + G_a \mathbf{u}_{Ga} \quad (4)$$

Where, when  $\Gamma > 0$ ,  $\mathbf{u}_{gl} = \mathbf{u}_l$ ; or  $\mathbf{u}_{gl} = \mathbf{u}_g$ ,  $\mathbf{u}_{Gs}$  and  $\mathbf{u}_{Ga}$  represents the velocity of steam and noncondensable air from the pipe break respectively,  $\Sigma$  is a stress tensor[11].

Momentum conservation for the continuous liquid water in the containment is written as

$$\begin{aligned} \frac{\partial}{\partial t} [(1 - \alpha) \rho_l \mathbf{u}_l] + \nabla \cdot [(1 - \alpha) \rho_l \mathbf{u}_l \mathbf{u}_l + (1 - \alpha) \Sigma_l] \\ = (1 - \alpha) \rho_l \mathbf{g} - \Gamma \mathbf{u}_{gl} + m \psi \mathbf{u}_l + G_l \mathbf{u}_{Gl} \end{aligned} \quad (5)$$

Where,  $\mathbf{u}_{Gl}$  represents the velocity of liquid from the pipe break.

For the assumption that the noncondensable air and the steam have the same temperature distribution, the energy conservation equation for the air and steam mixture will be written as

$$\begin{aligned} \frac{\partial}{\partial t} [\alpha (\rho_g h_g - p)] + \nabla \cdot [\alpha (\rho_g h_g - p) \mathbf{u}_g] + \alpha \nabla \cdot (\Sigma_g \mathbf{u}_g + \mathbf{q}_g + \mathbf{q}_{Tg}) \\ = p \frac{\partial \alpha}{\partial t} + q_{wg} \psi + q_{ig} + \Gamma h_{ss} - m \psi h_{ss} + G_s h_{Gs} \end{aligned} \quad (6)$$

Where,  $h_g$  represents specific enthalpy of gas mixture,  $q_{wg}$  is the wall heat flux from wall to gas,  $q_{ig}$  is the heat flux from the interface of saturated layer between liquid and steam to gas,  $h_{ss}$  is enthalpy of saturated steam,  $\mathbf{q}_g$  is heat flux vector of gas, and  $\mathbf{q}_{Tg}$  is the heat flux vector taking into account turbulence in gas mixture.

Energy conservation for the continuous liquid water is described as the following equation.

$$\begin{aligned} \frac{\partial}{\partial t} [(1 - \alpha) (\rho_l h_l - p)] + \nabla \cdot [(1 - \alpha) (\rho_l h_l - p) \mathbf{u}_l] + (1 - \alpha) \nabla \cdot (\Sigma_l \mathbf{u}_l + \mathbf{q}_l + \mathbf{q}_{Tl}) \\ = p \frac{\partial \alpha}{\partial t} + q_{wl} \psi + q_{il} - \Gamma h_{ls} + m \psi h_{ss} + G_l h_{Gl} \end{aligned} \quad (7)$$

Where,  $h_l$  represents specific enthalpy of fluid mixture,  $q_{wl}$  is the wall heat flux from wall to liquid,  $q_{il}$  is the heat flux from the interface of saturated layer between liquid and steam to liquid,  $h_{sl}$  is enthalpy of saturated liquid,  $\mathbf{q}_l$  is heat flux vector of liquid, and  $\mathbf{q}_{Tl}$  is the heat flux vector taking into account turbulence in liquid.

The models include the k- $\epsilon$  transport equation for the turbulence kinetic energy calculation and the turbulent dissipative rate equation for the main gas flow [12], which can be chosen to use in calculation. The transport equation for turbulent kinetic energy can be calculated by

$$\frac{\partial(\alpha\rho_g k)}{\partial t} + \nabla \cdot (\alpha\rho_g k \mathbf{u}_g) = \frac{\partial}{\partial X_j} \left[ \left( \mu + \mu_T \right) \frac{\partial k}{\partial X_j} \right] + 2\mu_T D_{kj} \frac{\partial u_{g,k}}{\partial X_j} - \alpha\rho_g \varepsilon \quad (8)$$

Transport equation for the turbulent dissipation rate equation can be written as

$$\begin{aligned} \frac{\partial(\alpha\rho_g \varepsilon)}{\partial t} + \nabla \cdot (\alpha\rho_g \varepsilon \mathbf{u}_g) = \\ \frac{\partial}{\partial X_j} \left[ \left( \mu + \frac{\mu_T}{\sigma_s} \right) \frac{\partial \varepsilon}{\partial X_j} \right] + C_{s1} \frac{\varepsilon}{k} \mu_T D_{ij} \frac{\partial u_{gi}}{\partial X_j} - C_{s2} \alpha\rho_g \frac{\varepsilon^2}{k} \end{aligned} \quad (9)$$

Where,  $C_{s1}=1.44$ ,  $C_{s2}=1.92$ , and  $\sigma_s=1.3$ .

With the combination of the above nine conservation equations, the pressure field, the velocity field and the temperature field of the fluid in the containment could be calculated. In the code, the above equations are discretized with staggered-mesh and finite volume method under cylindrical coordinate system for the fluid field in the containment.

### 2.3. Equation Solution on Heat and Mass Transfer in Containment

The PCCS performance is highly dependent upon the physical phenomena during the transient, so the analysis code for the design and evaluation on the PCCS is required to model the key thermal-hydraulic phenomena and process accurately, and its results will provide conservative predictions on the pressure response in the containment under the DBAs.

With order of importance in determining the containment pressure in a PIRT, the following important phenomena were determined:

- Condensation mass transfer inside containment shell
- Evaporation mass transfer outside containment shell
- Convective air flow rate
- Heat conduction in the containment shell
- Condensation on the internal heat sinks

For the evaluation on the PCCS performance, it needs the analysis code satisfies the requirement to model and simulate the transient heat & mass transfer processes mentioned above.

#### 2.3.1. Equation on heat and mass transfer

The heat transfer path from the reactor to the environment during the postulated accident is illustrated as Figure 2.

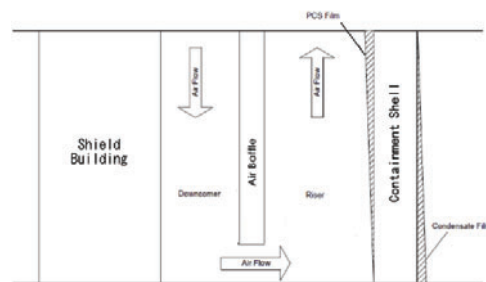


**Figure 2. Heat Transmission of PCCS**

Generally, heat conduction exists in the steel containment shell and the flowing water film, and heat and mass transfer exists on the interface of fluid.

The heat conduction in containment shell can be simplified to one-dimensional heat conduction, so the wall conduction equation would be:

$$\frac{\partial T_{shell}}{\partial t} = \frac{\lambda_{shell}}{\rho_{shell} c_{p,shell}} \frac{\partial^2 T_{shell}}{\partial x^2} \quad (10)$$

Where,  $T_{shell}$  is temperature of the containment shell,  $\lambda_{shell}$  is thermal conductivity of the containment shell,  $C_{p,shell}$  is specific heat of the containment shell,  $\rho_{shell}$  is density of the containment shell,  $x$  represents the direction normal to the surface of the containment. On the interface of the containment and the water film, the surface temperature of the containment is equal to the inside surface water film. The boundary condition is written as:

$$T_{shell}|_{interface} = T_{film}|_{interface} \quad (11)$$

The energy in the water film should balance with the heat from the wall into the film, the heat conduction through the film, and the heat transfer from the surface of the water film to the bulk gas, and the energy change caused by the water film flowing. For the water film thickness is small, the water film along the outside surface of containment shell and the heat conduction across the water film will be considered as one-dimensional flow and one-dimensional heat transfer, where the viscous dissipation term will be neglected. The general energy transfer equation for the flowing water film can be written in terms of temperature as

$$\frac{\partial T_{film}}{\partial t} = \frac{\lambda_{film}}{\rho_{film} c_{p,film}} \frac{\partial^2 T_{film}}{\partial x_{film}^2} + u_z \frac{\partial T_{film}}{\partial z} \quad (12)$$

Where,  $T_{film}$  is temperature of the water film,  $C_{p,film}$  is specific heat of the water film,  $\rho_{film}$  is density of the water film,  $u_z$  is flow velocity of the water film on the surface of the containment shell, and  $z$  represents the direction along a meridian from the containment top.

The heat and mass transfer on the surface of the water film combines evaporation, condensation, convection and radiation. The water film will evaporate on the outside surface of the containment or condensate on the inside surface of the containment. The boundary energy equation of the water film surface is:

$$\lambda_{film} \frac{\partial T_{film}}{\partial x} \Big|_{surf} = q_{convection} + q_{evaporation} + q_{condensation} + q_{radiation} \quad (13)$$

Where,  $q_{convection}$  is heat flux by convection between the outside surface of the water film and the flowing air, it can be written as

$$q_{convection} = H_c (T_{film,surf} - T_{air}) \quad (14)$$

Where,  $H_c$  is heat transfer coefficient,  $T_{film,surf}$  is the outside surface temperature of the water film,  $T_{air}$  is the bulk air temperature

$q_{evaporation}$  is the heat transferred by evaporation from the outside surface of the water film, it can be calculated by the following Eq. (15), while  $q_{condensation}$  has the similar formation.

$$q_{evaporation} = h_{fg} K_m (P_{film}^{steam} - P_{air}^{steam}) \quad (15)$$

Where,  $K_m$  is mass transfer coefficient,  $h_{fg}$  is latent heat of vaporization of the water film,  $P_{air}^{steam}$  is partial pressure of steam in the near air,  $P_{film}^{steam}$  is saturation pressure under the temperature of the water film surface.

$q_{radiation}$  is the heat transferred by radiation from the outside surface of the water film to the inside surface of the air baffle, it can be written as

$$q_{radiation} = \varepsilon \kappa (T_{film,surf}^4 - T_{baffle,surf}^4) \quad (16)$$

Where,  $T_{baffle,surf}$  is the inside surface temperature of the air baffle,  $\varepsilon$  is Stefan-Boltzman constant,  $5.6697 \times 10^{-8} \text{W/m}^2 \cdot \text{K}^4$ ,  $\kappa$  is emissivity of the water film surface.

The heat transfer from the inside of the containment could be solved with the equations (10)-(13). For numerical computation, these equations will be discretized further.

Analogously, the heat transfer on the inside surface of the air baffle, the heat conduction in the air baffle, the heat transfer on the outside surface of the air baffle, the heat transfer on the inside surface of the shield building, the heat conduction in the shield building, and the heat transfer from the outside surface of the shield building to the ambient environment can be described by the similar energy equations also.

### 2.3.2. Equation on the flowing water film on the containment

Liquid-film tracking model [13] is used in the code to describe the flowing water film on the inside and outside surface of the containment shell, whose thickness and temperature is time-dependent. For the thin thickness of water film on the containment surface, the equation can be simplified as

$$\rho_l \frac{\partial \delta}{\partial t} + \rho_l u_z \frac{\partial \delta}{\partial z} = m \quad (17)$$

Where,  $\delta$  is the thickness of water film.

By the liquid-film tracking model, the time-dependent water film flowing on the inside or outside surface of the containment due to evaporation or condensation could be calculated.

### 2.3.3. Main correlations on heat and mass transfer

#### (a) Condensation

As the results of the PIRT analysis mentioned above, the dominant phenomena is heat and mass transfer, including condensation on the inside surface of the containment shell and evaporation on the outside of the containment shell, so these heat transfer correlations are important for the PCCS transient analysis. In the code, three typical empirical correlations could be chosen for modeling the heat transfer on the surface of the structures (the internal heat sinks in containment and the containment shell): Uchida correlation [14], Gido-Koestl correlation [15], and Tagami correlation [16]. These correlations are intended for use in containment analysis codes based on conservation equations written for a single large control volume representing the entire containment. However, it is hopeless to get finer detail on the flow field in the containment. Treating the containment interiors as a single volume cannot achieve explicit results on the distribution of noncondensables and the surface temperature and heat flux distributions which are required in the current containment analysis. In fact, heat and mass transfer with the structures governed by local conditions within the given boundary layer should be correlated to conditions as near the boundary layer as possible. Therefore, a methodology of heat mass transfer analogy was developed, which includes a more complete formulation of the thermal-hydraulic equations linked with correlations based on bulk fluid conditions relatively near a surface to provide spatially distributed conditions within containment. Heat transfer is driven by temperature gradient, and mass transfer is driven by concentration gradient. The correlation of mass transfer is similar with heat transfer. The mass flux based on the difference of the pressure can be derived with analog[17]. The heat and mass transfer model based the above methodology is also provided in this code, where steam and noncondensables within the containment can be separately tracked and fluid conditions in the regions near the structures are available.

#### (b) Convection

The flow regime in large containment will primarily be turbulent rather than laminar. The heat transfer in the containment is free convection and the heat transfer in the annulus between the containment and the air baffle is the mixed convection.

For laminar free convection heat transfer, the correlation [18] is used

$$Nu_{free} = 0.27(Gr Pr)^{1/4} \quad (18)$$

Where, Gr is Grashof number, Pr is Prandtl number.

For turbulent free convection heat transfer, the McAdams correlation [19] is used.

$$Nu_{free} = 0.13(Gr Pr)^{1/3} \quad (19)$$

For turbulent forced convection heat transfer, the correlation [20] is used.

$$Nu_{force} = 0.037 Re^{4/5} Pr^{1/3} \quad (20)$$

Where, Re is Reynolds number.

### 3. ANALYSES ON CONTAINMENT TRANSIENT

The thermal-hydraulic transients in the containment with the PCCS performance are not identical under different scenarios, which is not only affected with the PCCS design, but also with the different boundary conditions and initial conditions in the scenarios.

For better understanding the PCCS performance under the postulated accidents, the analyses on the PCCS of the AP1000 under the postulated cold-leg LOCA and MSLB are carried out.

#### 3.1. Model and Claim

The 3D mesh division in model dominates the number of space cells in containment, and it will affect the calculation result on the thermal-hydraulic transient in containment. Finer mesh division will enhance the accuracy of the calculation result, but consume more time and cost. With the balance of both sides, the 16×6×6 mesh division is selected used in the analysis for AP1000(16 meshes in vertical direction, 6 meshes in radial direction and 6 meshes in the angular direction). The containment model under cylindrical coordinate system is shown as Figure 3. The space cells in the dome of the containment are divided automatically under cylindrical coordinate system in the code to ensure the same free volume with the real one. The main internal structures in the containment are considered in the model as heat sink, such as vessels and pipes, concrete cavity, and so on. The mass and energy of the fluid released from the reactor under the postulated LOCA or MSLB is calculated by a general thermal-hydraulic system code RELAP5 and expressed an input as the boundary condition. According the actual operation condition, the initial conditions which are assumed conservatively in the reference case, are listed as Table I.

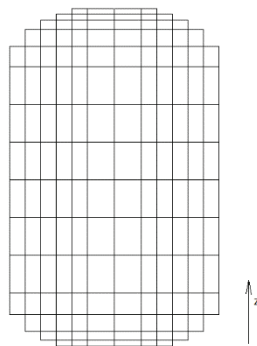


**Figure 3. Containment Mesh Division in the Model**

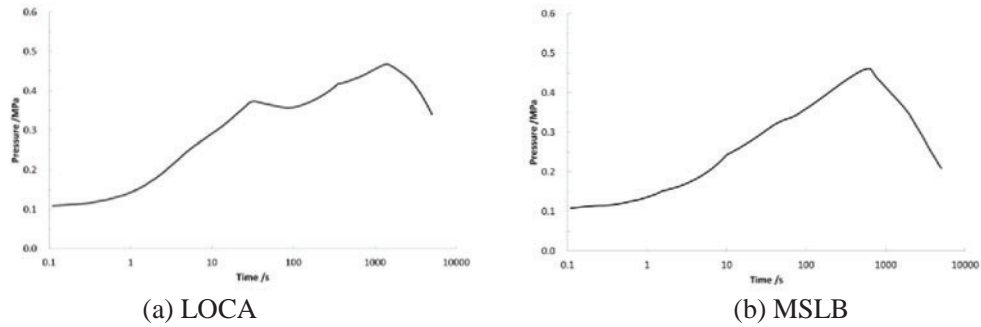
**Table I. Parameters in the reference case**

Parameters	Reference value
Initial temperature in containment(°C)	49
Initial pressure in containment(MPa)	0.107
Initial relative humidity in containment (%)	0
Ambient temperature(°C)	46
Ambient pressure(MPa)	0.101
Ambient relative humidity (%)	100
Water film temperature(°C)	49

#### 3.2. Results in the Reference Case

The pressure transients in the steel containment during the postulated cold-leg LOCA and MSLB are considered to be very important for the evaluation of the PCCS performance.

After the coolant spouts out from the pressure vessel or the main steam line into the containment, the pressure in the containment will increase at the early stage of the postulated transient, and then decreases gradually with the PCCS performance. The transient pressure of the reference case under cold-leg LOCA and MSLB calculated by PCCSAP-3D is shown in Figure 4. The results show that the maximum of the pressures in the containment during LOCA and MSLB are 0.467MPa and 0.461MPa, which are both limited under the pressure design value of the AP1000 containment and the containment is cooled effectively by the PCCS performance.

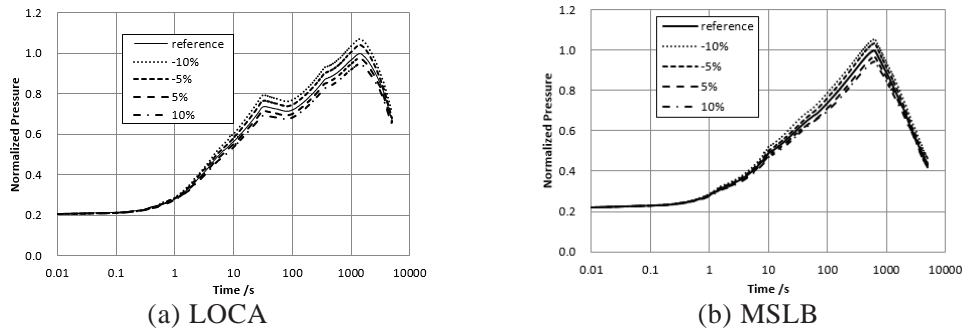


(a) LOCA (b) MSLB  
**Figure 4. Containment Pressure during LOCA and MSLB**

### 3.3. Calculation and Analysis

#### 3.3.1. Free volume in containment

The steel containment, which provides protection entirely for a nuclear power plant and contain the radioactive isotopes, will hold all the released water and gas from the reactor during the postulated LOCA or MSLB. It is obvious that the transient pressure inside the containment is influenced by the free volume of the containment. For the certain blown-down transient, larger the free volume is, lower the pressure peak is. The pressure transients with different free volumes under the postulated LOCA and MSLB are compared in Figure 5. With 10 percent change on the free volume relative to the reference case, the maximal pressure under the postulated accident will change prox. 7%.



(a) LOCA (b) MSLB  
**Figure 5. Different Free Volume of Containment**

#### 3.3.2. Thickness of containment shell

The containment shell will absorb heat from the water/steam spouting from the reactor at the early stage of the postulated accident, which will constrain the pressure increase of the containment. Larger thickness of the containment shell will enhance its heat capacity, so the peak pressure decreases with the increase of the containment thickness (Figure 6). Although

larger thickness of the containment shell will increase its heat resistance on the other side, the influence is not dominant for the excellent heat conductivity of the steel shell.

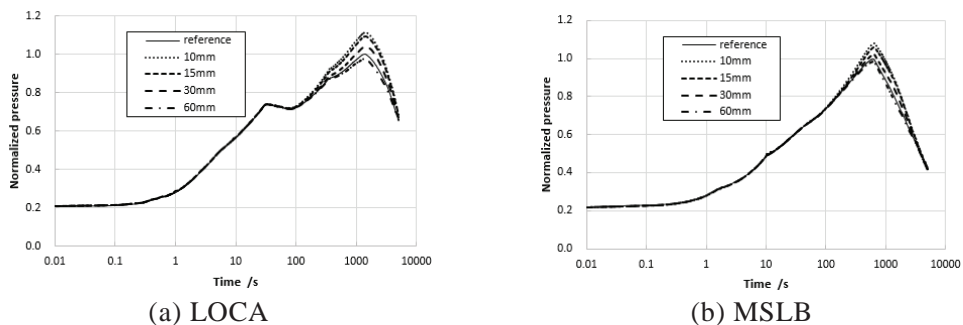


Figure 6. Different Containment Thickness

### 3.3.3. Initial temperature in containment

The initial temperature in the containment means the average temperature of air in the containment in normal steady operation. In the analysis, the initial temperatures of the structures in the containment are also assumed to be same with of the initial air temperature in the containment for energy balance.

The transient will be affected by heat and mass transfer in the steel containment shell and the heat capacity of the internal structures in the containment.

Several cases in a large range of the initial containment temperature from 10°C to 49°C are selected to be analyzed in Figure 7. The transient with the initial containment temperature(49°C) is used in the reference case, and other cases are normalized to compare with it. The pressure with lower temperature is a little higher than that in the reference case at the beginning of the transient because larger mass of air exists in the containment. But the latter exceeds the former gradually and gets the higher peak pressure because of the structures in the containment which function as heat sink. The maximal pressure in the case(10°C) is 6% less than that in the reference case under the postulated LOCA, and is 5% less than that in the reference case under the postulated MSLB.

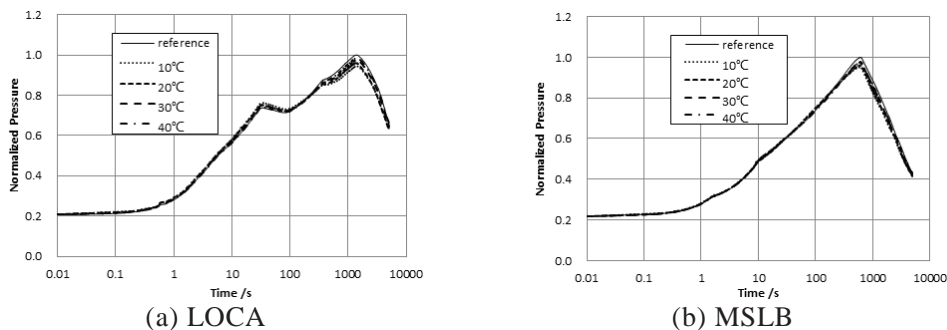


Figure 7. Different Initial Temperature in Containment

### 3.3.4. Initial humidity in containment

The initial humidity in the containment will influence the steam condensation on the surface of the steel containment and the internal structures. Higher relative humidity means lower concentration of noncondensable air in the containment, which will strengthen the heat and mass transfer on the surfaces. The minimum of initial relative humidity in containment (0 percent) is used in the reference evaluation case, which results in a higher peak pressure. Other cases are normalized to compare with the reference case in Figure 8. The result shows

agreement with the above analysis. But the effect of the initial relative humidity is limited during the accident transients. Compared with the reference case, the reduction of the peak pressure during the accident in other cases is less than 3%, even with 100% initial relative humidity in containment.

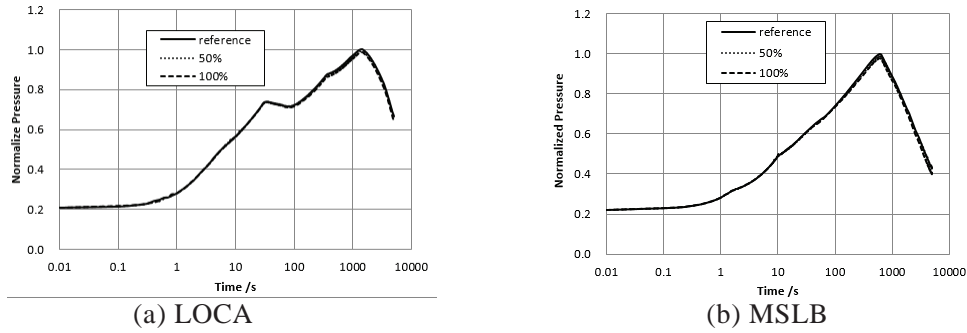


Figure 8. Different Initial Humidity in Containment

### 3.3.5. Initial ambient temperature

The initial ambient temperature refers to the initial temperature of the bulk air flowing in the annulus between the steel containment shell and the air baffle. Most of heat energy will be removed to environment with the flowing air in the annular channel by natural and forced convection, which is dependent on the temperature difference between the water film and the bulk air in the annulus. Obviously, lower ambient air temperature will increase the buoyancy of air flow and heat transfer capacity. The initial ambient temperature(46°C) is used in the reference evaluation case, and the normalized comparison is shown in Figure 9. The lower initial ambient temperature will reduce the peak pressure during the postulated LOCA and MSLB, but its influence is not significant. It can be explained by the reasons that the ambient temperature performs a limited effect in the convection and the heat removal by convection just provides a limited contribution in the total energy removal from the containment.

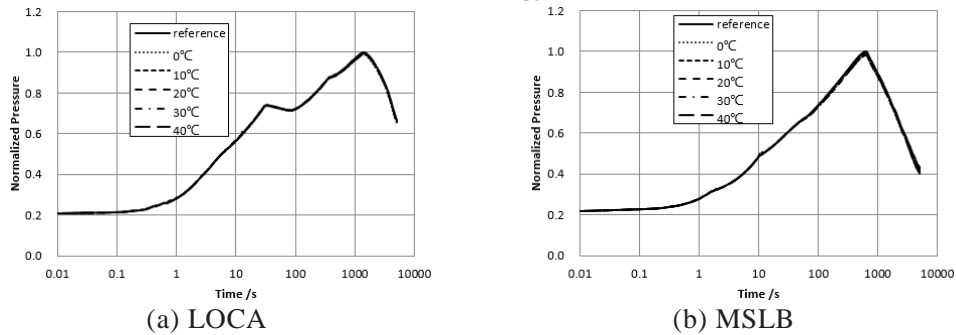


Figure 9. Different Initial Ambient Temperature

### 3.3.6. Initial ambient humidity

Figure 10 illustrates the normalized comparison with different initial ambient humidity. The evaporation of the water film on the outside surface of the steel containment shell is related with the relative humidity of the air flowing through the annular channel between the containment shell and the air baffle. Higher relative humidity means that higher vapor partial pressure in the ambient air will restrain the evaporation of water film, which result in the decrease of heat removal from the containment and the increase of the pressure during the postulated accident. But the vapor concentration in the bulk air mixture is small, in

comparison with that at the water film interface. Therefore, the ambient humidity has no obvious effect on the evaporation.

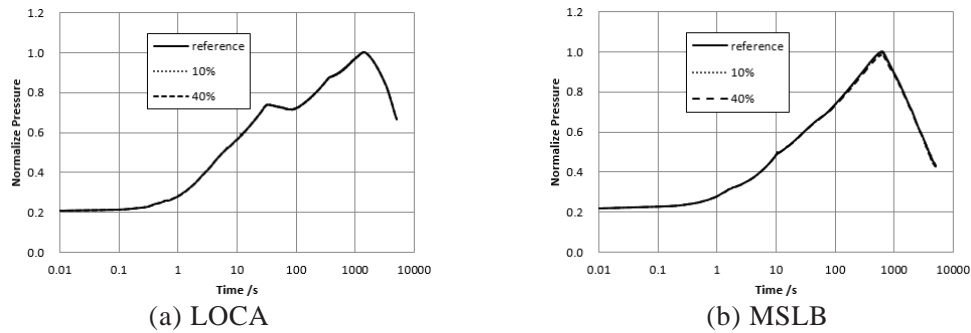


Figure 10. Different Initial Ambient Humidity

### 3.3.7. Heat and mass transfer model

The PCCS transient will be affected by the condensation on the inside surface of the steel containment and the heat structures in the containment, and also by the evaporation of water film on the outside surface of the steel containment. Different correlations used in the simulation code to model the heat and mass transfer of condensation/evaporation may result in different pressure transients. In the code, water film track model will be applied for condensation/evaporation on the surface of the steel containment. And several models, such as Uchida, Gido, Tagami and heat and mass transfer analogy, can be chosen for the condensation on the surface of the internal heat structures in the containment. The Uchida model is used for the heat and mass transfer on the internal structures in the reference case to have a normalized comparison with other models. As shown in Figure 11, no obvious differences are observed in the results, which indicates that the condensation on the surface of the internal structures may not be a governing phenomenon in the PCCS performance.

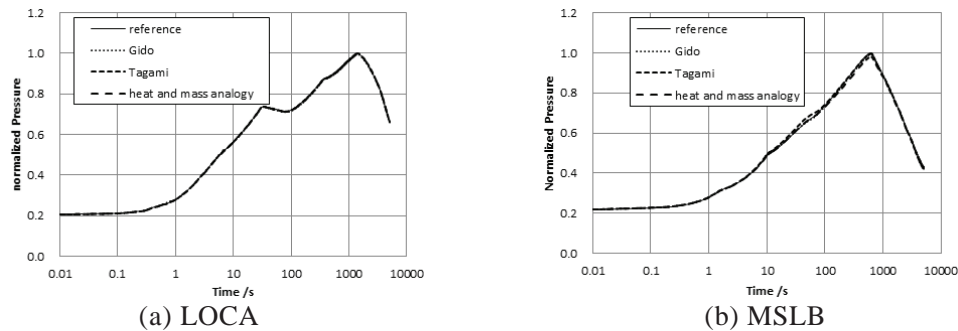


Figure 11. Different Heat and Mass Transfer Model

### 3.3.8. Mass flow rate of cooling water from PCCWST

During the PCCS performance, the water in the PCCWST will be sprayed on the outside surface of the steel containment shell and form water film to cool the containment. The heat transfer on the containment will be weakened when the water film evaporates to dry out. Figure 12 show that the transient pressure under the postulated LOCA and MSLB with different mass flow rate of cooling water released from the PCCWST, and the change of the mass flow rate in LOCA has a little more significant effect on the pressure than that in MSLB. It is because that the heat from the containment in LOCA are much larger than that in MSLB, and the evaporation of water film on the shell in LOCA is stronger than that in MSLB, which affects the location where the water film on the containment dries out. Fortunately, with the

comparison result, the pressure response under the postulated DBAs is not sensitive with the mass flow rate of cooling water, which indicates the current design on the mass flow rate of cooling water from the PCCWST is enough conservative for the PCCS performance.

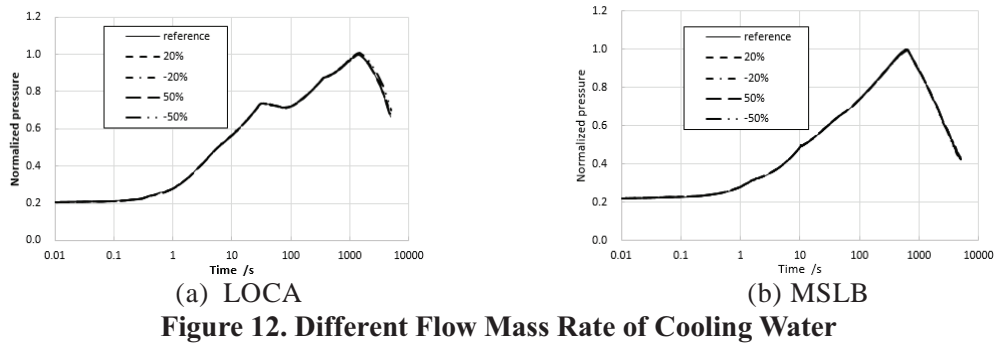


Figure 12. Different Flow Mass Rate of Cooling Water

### 3.4. Sensitivity Comparison

A series of analyses is carried out to study the effect of some factors on the pressure response under the postulated DBA for the AP1000 PCCS performance, and its comparison is shown as Figure 13. The results show that the containment parameters have dominant effect on the pressure response, in comparison with the initial conditions. 10% change on the free volume of the containment will result in 7% change on the peak pressure, 50% change on the thickness of the containment shell will also result in 7% change on the peak pressure under LOCA. The effect of the initial conditions on the pressure response is generally less than 3%. The initial conditions in the containment including the temperature and the relative humidity in the containment have more significant effect than the ambient temperature and the ambient humidity.

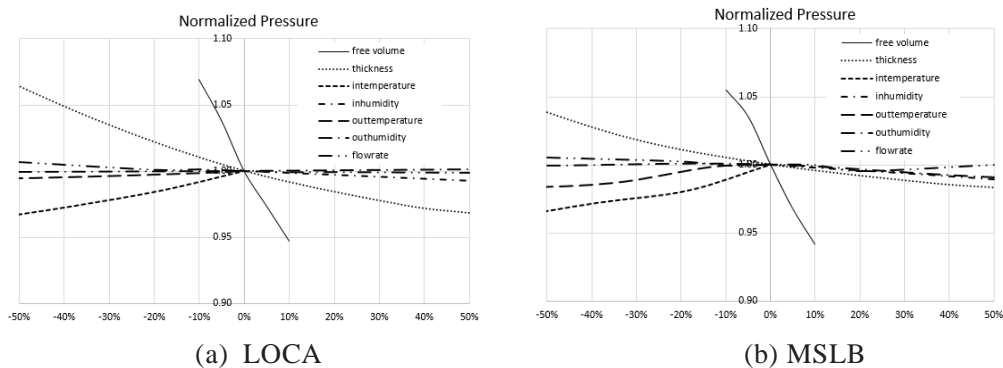


Figure 13. Sensitivity Comparison

## 4. CONCLUSIONS

The passive containment cooling system is one main passive safety component of the advanced pressurized water reactor to remove heat released from reactor system in the postulated DBA event. It is significant to simulate and analyze the transient of the PCCS performance.

The pressure response in the containment is the most important for the evaluation on the PCCS performance. A dedicated code PCCSAP-3D for the PCCS analysis was used for the research on the pressure response under the postulated LOCA and MSLB. The analysis show that the free volume and the shell thickness of the containment are dominant for the containment pressure response, in comparison with the initial conditions. The effects of the

initial conditions in the containment are greater than the ambient initial conditions, but its effect on the maximal pressure is less than 3%, even with 50% change of the reference value.

## ACKNOWLEDGMENTS

Thanks for cooperation received from State Nuclear Power Technology R&D Center and support from Dr. Jiyang YU and Dr. Baoshan JIA of the Engineering Physics Department of Tsinghua University.

## REFERENCES

- 1) Lin Chengge, and Yu Zusheng, *The Nuclear Power Plant Technology on Advanced Passive Pressurized Water Reactor*, Atomic Energy Press, (2010).
- 2) Lin Chengge, Yu Zusheng, and Ou Yangyu, *An Advanced Passive Plant API000*, Atomic Energy Press, (2008).
- 3) Frank Rahn, *GOTHIC Containment Analysis Package Technical Manual*, EPRI, (2009).
- 4) Y. D. Hwang, and B. D. chung, B. H. Cho, "PCCS Analysis Model for the Passively Cooled Steel Containment", *Journal of the Korean Nuclear Society*, **30**[1], 26–39(1998).
- 5) Sun, J. G., Chien, T. H., and Sha, W. T, "Validation of COMMIX with Westinghouse AP600 PCCS test data", *Nuclear Safety*, **36**[2], 310–320(1995).
- 6) Zhangdi, and Yan Jinqun, "Approach and Method to Use WGOthic Code Distributed Parameter Model in Containment Integrity Analysis," *The 12th thermal hydraulics conference*. Lijiang, China, September 14-15,(2011).
- 7) Lin Chengge, Zhao Ruichang, and Liu Zhitao, "Containment integrity analysis under accidents", *Chinese Journal of Nuclear Science and Engineering*, **30**[6], 181-192(2010).
- 8) Yu, J., Jia, B., "PCCSAC: A Three-Dimensional Code for AC600 Passive Containment Cooling System Analysis", *Nuclear Science and Engineering*, **142**[2], 230-236 (2002).
- 9) Wang Yan, Zhou Zhiwei, "A Code Development for the Passive Containment Cooling System Analysis of the Advanced PWR in China"(N9P0082), *The 9th International Topical Meeting on Nuclear Thermal-Hydraulics, Operation and Safety (NUTHOS-9)*, Kaohsiung, Taiwan, September 9-13,( 2012).
- 10) Zhang Yaoli, Yang Yanning, Zhou Zhiwei, et al., "Improvement on algorithm for pressure equation in PCCSAP-3D", *Chinese Journal of Computational Physics*, **29**[5], 699-706(2012).
- 11) Warsi, Z. U. A, *Fluid Dynamics – Theoretical and Computational Approaches*, CRC Press, Inc, (1993).
- 12) Launder, B.E., Spalding, D.B, "The numerical computation of turbulent flows". *Computer method in applied mechanics and engineering*, **3**, 269-89(1974).
- 13) Schlichting H. *Boundary-Layer Theory, seventh edition*, McGraw-Hill, 235(1978).
- 14) H. UCHIDA, A. OYAMA, and Y. TOGO, "Evaluation of Post-Incident Cooling Systems of Light-Water Power Reactors," *Proceedings of International Conference on Peaceful Uses of Atomic Energy*, 93-102(1965).
- 15) Gido R G, and Koestel A, "Containment Condensing Heat Transfer", Los Alamos National Lab.25(1983).
- 16) T. TAGAMI, "Interim Report on Safety Assessments and Facilities Establishment Project for June 1965, No. 1", Japanese Atomic Energy Research Agency, unpublished.
- 17) E. R. G. Eckert, and R. M. Drake. Jr., *Analysis of Heat and Mass Transfer*, McGraw-Hill, (1972).
- 18) Holman J P. *Heat transfer*, 9th ed., McGraw-Hill, (2002).
- 19) Mcadams W H, *Heat transmission*, McGraw-Hill, (1954).
- 20) F. P. Incropera and D. P. DeWitt, *Introduction to Heat Transfer*, 3rd ed., John Wiley and Sons, Inc, (1996).